Desalination and Water Treatment
www.deswater.com
doi: 10.1080/19443994.2014.958538

56 (2015) 2092–2104
November

Taylor & Francis
Taylor & Francis Group

Effective removal of As (III) from drinking water samples by chitosan-coated magnetic nanoparticles

M. Abdollahi[a], S. Zeinali[a,b,*], S. Nasirimoghaddam[a], S. Sabbaghi[a,b]

[a]*Faculty of Advanced Technologies, Department of Nanochemical Engineering, Shiraz University, Shiraz, Iran, Tel. +989183451911; email: maryamabdolahi20@yahoo.com (M. Abdollahi), Tel. +987113769; email: zeinali@shirazu.ac.ir (S. Zeinali), Tel. +989139956257; email: snm_karmania@yahoo.com (S. Nasirimoghaddam), Tel. +987116133709; email: sabaghi@shirazu.ac.ir (S. Sabbaghi)*
[b]*Nanotechnology Research Institute, Shiraz University, Shiraz, Iran*

Received 20 January 2014; Accepted 15 August 2014

ABSTRACT

Chitosan-coated Fe_3O_4 nanoparticles were developed with the purpose of removing arsenic from aqueous solution. Chitosan was first carboxymethylated and then covalently bounded on the surface of Fe_3O_4 nanoparticles via carbodiimide activation. The grafted chitosan on the Fe_3O_4 nanoparticles contributed to the enhancement of the adsorption capacity, because of the strong ability of chitosan's multiple hydroxyl and amino groups to adsorb arsenic. The prepared magnetic adsorbent was characterized by Transmission electron microscopy (TEM), vibrating sample magnetometer, and Fourier transform infrared. The characterization results showed that chitosan is grafted onto Fe_3O_4 nanoparticles. TEM micrographs showed that the chitosan-coated Fe_3O_4 nanoparticles were monodispersed and had a mean diameter lower than 10 nm. The chitosan-coated Fe_3O_4 nanoparticles exhibit superparamagnetic properties at room temperature and saturation magnetization equaled $50\,\mu g^{-1}$. To achieve the highest efficiency in absorption experiments, the effect of some influential parameters on the arsenic removal such as pH, dosage of adsorbent, and contact time were evaluated. The adsorption data obeyed the Langmuir equation with a maximum adsorption capacity of $10.5\,mg\,g^{-1}$ for arsenic (III) at pH 9 and at room temperature. This material can be used for arsenic adsorption from water and wastewater, and can be easily separated by applied magnetic field. This nanoadsorbent can reduce arsenic concentration to under the allowed limit declared by the World Health Organization.

Keywords: Arsenic removal; Drinking water treatment; Magnetic nanoparticle; Chitosan

1. Introduction

Arsenic (As), one of the common constituent of earth crust, is a contaminant of groundwater and surface water resources. Arsenic is classified as one of the most toxic and carcinogenic chemical elements. The most commonly existing forms of arsenic species in aqueous environments include arsenate (as AsO_4^{3-}(V)) in well-oxidized waters and arsenite (as AsO_2^-(III)) in reduced environments. Trivalent arsenic or arsenate is more toxic and more mobile than the pentavalent form (arsenite) in the environment [1]. Arsenic is present in water as a result of both natural and anthropogenic activities. The main natural source of arsenic is

*Corresponding author.

dissolution of arsenic-rich rocks. Arsenic may also be resulted from industrial and mine waste discharges [2]. Arsenic pollution has been reported recently in USA, China, Chile, Bangladesh, Argentina, Japan, India, Thailand, and Islamic Republic of Iran [3,4]. Exposure to arsenic-contaminated water can lead to a number of health problems such as gastrointestinal symptom, disturbance of cardiovascular and nervous system function, pigmentation, depigmentation, causes cancer of the bladder, lungs, skin, kidney, liver, and prostate [5,6]. The US Environmental Protection Agency and the World Health Organization (WHO) had adopted a maximum permissible contaminant level of 10 ppb for arsenic in drinking water as the standard, considering the epidemiological evidence of arsenic carcinogenicity [7]. Treatment processes including precipitation, membrane separation, ion exchange, microbial transformation [8–11], and adsorption have been used for arsenic removal from contaminated water resources. These methods are effective in removing arsenate without any pretreatment step, but this step usually is needed for arsenite removal. Another drawback of these methods is that they produce large amounts of toxic sludge which needs further treatment before disposal into the environment [12]. The adsorption from solution as a treatment method is one of the most effective and inexpensive methods which has received more attention recently [13]. In this treatment method, many types of adsorbents have been used for arsenic removal [14]. Therefore, in adsorption-based technologies, development of highly effective adsorbents is of great importance [15]. Recently, Fe_3O_4 based adsorbents have widely been used in adsorption due to their specific characteristics [16]. Magnetic nanoadsorbents enjoy the properties of both magnetic separation and nanosized materials, thus can be easily separated with an external magnetic field [17]. In addition, the use of magnetic field for separating adsorbents is more selective and efficient than centrifugation and filtration [1]. The surface functionality of Fe_3O_4 nanoparticles was achieved through coating it by natural or synthetic polymers. Chitosan is a natural polyaminosaccharide, synthesized from the de-N-acetylation of chitin. Chitin is the world's second most abundant natural polymer after cellulose, which makes up the shells of crustaceans such as crabs, prawns, insects, and shrimps. Chitosan is biodegradable, biocompatible, nontoxic, and abundant in nature, making it an environmental friendly substance [13,18]. Chitosan can be used as an adsorbent to remove heavy metals due to the presence of a large number of amino and hydroxyl groups, which have high activity as adsorption sites. Several studies have illustrated that chitosan and its derivatives could be effective in arsenic removal from aqueous solutions [12,19]. Chitosan-coated Fe_3O_4 nanoparticles provide a promising single-step treatment option to treat arsenic-contaminated natural water. The high surface area-to-volume ratio of the Fe_3O_4 nanoparticles and magnetic properties together with the adsorption capabilities of chitosan would facilitate the removal of arsenic from wastewater.

In this work, Fe_3O_4 magnetic nanoparticles were functionalized with Chitosan to synthesize a novel magnetic nanoadsorbent for the adsorption of arsenic contamination. The size, morphology, and properties of the Chitosan-coated magnetic nanoparticles were characterized using different analytical tools. The chitosan-coated Fe_3O_4 nanoparticles are monodisperse and have a diameter lower than 10 nm. They exhibit superparamagnetic properties at room temperature and saturation magnetization equaled 50 μg^{-1}. Besides the effect of several factors such as pH, initial arsenic concentration, and contact time on arsenic removal, the adsorption isotherm was also studied. In Iran, it has been reported that there is arsenic contamination in groundwater sources in many western and northwestern areas especially in Kurdistan province [4,20]. Real water samples were gathered from Kurdestan villages to investigate the ability of chitosan-coated Fe_3O_4 nanoparticles in removing arsenic in these samples.

2. Experimental

2.1. Materials

Iron (II) chloride tetrahydrate, iron (III) chloride hexahydrate, sodium hydroxide (NaOH), ammonium hydroxide (25%), chitosan, chloroacetic acid, carbodiimides (cyanamide, CH_2N_2), arsenic trioxide (As_2O_3), and ethanol (99%) were purchased from Merck. All chemicals were the guaranteed or analytic grade reagents commercially available and used without further purification.

2.2. Synthesis of chitosan-coated magnetic nanoparticles

First, chitosan was carboxymethylated according to the methods reported in the literature [21]. Briefly, 1 g chitosan and 5 g sodium hydroxide were added into 34 mL of isopropanol/water (80/20) mixture at 60°C to swell and alkalize for an hour. Then, 6.6 mL of monochloroacetic acid solution (0.75 gmL^{-1} in isopropanol) was added into the reaction mixture drop by drop in 30 min. After keeping the reaction mixture at the same temperature for 4 h, 67 mL of ethanol (70%)

was added to stop the reaction. Finally, the solid was filtered, rinsed with 70 and 99% ethyl alcohol to desalt and dewater, and then it was dried in oven at 50˚C.

Then, magnetite nanoparticles were prepared by chemical coprecipitation method. In brief, a complete precipitation of Fe_3O_4 was achieved under alkaline condition, while maintaining a molar ratio of Fe^{2+}: Fe^{+3} = 1:2. In a typical synthesis to obtain 1 g Fe_3O_4 precipitate, 0.86 g of $FeCl_2{\cdot}4H_2O$ and 2.36 g of $FeCl_3{\cdot}6H_2O$ were dissolved in 40 mL of distilled water with vigorous stirring at a speed of 1,000 rpm. Five milliliter of NH_4OH (25%) was added after the solution was heated to 80˚C. The reaction was continued for 30 min at 80˚C under constant stirring to ensure the complete growth of the nanoparticle crystals. The resulting particles were then washed with distilled water at least five times to remove any unreacted chemicals and were dried in oven at 70˚C. For the grafting of carboxymethyl chitosan, 100 mg of magnetic nanoparticles were first added to 2 mL of buffer A (0.003 M phosphate, pH 6, 0.1 M NaCl), and the reaction mixture was sonicated for 10 min after adding 0.5 mL of carbodiimide solution (0.025 gmL^{-1} in buffer A). Finally, 2.5 mL of carboxymethyl chitosan solution (50 mg mL^{-1} in buffer A) was added and the reaction mixture was sonicated for another 60 min. The resulting nanoparticles were recovered from the reaction mixture using a permanent magnet and washed with water and ethanol, then dried in an oven at 70˚C.

2.3. Characterization methods

The size and morphology of chitosan-coated magnetic nanoparticles were observed by transmission electron microscopy (TEM Model- CM10 Philips Company). The size and size distribution of nanoparticles were measured by particle size analyzer on the HORIBA L-550 model. To confirm the existence of the surface coating, Fourier transform infrared (FTIR) spectroscopy measurements were performed on the RX1 model (Perkin-Elmer Company) using KBr as background over the range of 4,000–350 cm^{-1}. To investigate the magnetic properties of the Fe_3O_4 nanoparticles coated with chitosan, vibrating sample magnetometer (VSM, magnetic daghigh Kavir Company) at room temperature in the applied magnetic field from −10,000G to 10,000G was used.

2.4. Adsorption experiments

Arsenic removal by chitosan-coated magnetic nanoparticles was carried out in aqueous solutions by mixing 30 mg sorbent with 5 mL As(III) solution. The solutions of As(III) were obtained by dissolving arsenic trioxide (As_2O_3) into boiling distilled water. The effects of contact time, initial arsenic concentration, initial pH value, and adsorbent dose on the removal efficiency were investigated. When investigating the effect of solution's pH on arsenic adsorption, the initial As(III) concentrations in the solution were 50 ppm and the solution pH values were changed from 8 to 11. The pH value was adjusted using 1 mol L^{-1} NaOH solution. After completing the adsorption process, magnetic nanoparticles were removed magnetically from arsenic solution using a strong permanent magnet and the supernatant was collected. The concentrations of As(III) in supernatant solution were measured using the inductively coupled plasma-optical emission spectroscopy ICP-OES while the concentration of As(III) in the real samples was measured by inductively coupled plasma-mass spectrometry (ICP-MS). In order to determine the effectiveness of chitosan as coating, the adsorption of As(III) by the naked Fe_3O_4 nanoparticles was also investigated. The adsorption isotherm experiments were performed with different initial As(III) concentrations of the solutions by adding a constant dose of the chitosan-coated magnetic nanoparticles of 6 mg mL^{-1}.

The adsorption capacity (q_e, mg g^{-1}) of chitosan-coated magnetic nanoparticles were calculated using the following equation:

$$q_e = \frac{(C_0 - C_e)V}{m} \tag{1}$$

Also, the removal efficiency (E) of arsenic determined by next equation is as follows:

$$E(\%) = \frac{(C_0 - C_e)}{C_0} \times 100 \tag{2}$$

where C_0 and C_e are the initial and equilibrium concentrations (mg L^{-1}) of As(III) solution, respectively; V is the volume of the As(III) solution; and m is the weight of the chitosan-coated magnetic nanoparticles.

2.5. Kinetic experiments

Adsorption kinetic of As(III) on chitosan-coated magnetic nanoparticles was examined at room temperature with a constant concentration of 50 ppm of As(III) in different contact times. The experimental data of adsorption for As (III) onto chitosan-coated magnetic nanoparticles were analyzed using

Lagergren pseudo-first-order and pseudo-second-order kinetic models [15]. The correlation coefficient R^2 was utilized to express the uniformity between the experimental data and model-predicted values. A pseudo-first-order kinetic model is given through the following equation:

$$\ln(q_e - q_t) = \ln q_e - k_1 t \tag{3}$$

where q_e and q_t are the amounts of arsenic adsorbed by each unit of chitosan-coated magnetic nanoparticles at equilibrium state and time t, respectively (mg g^{-1}), k_1 is the pseudo-first-order rate constant and can be obtained from the plots of ln $(q_e - q_t)$ against t. A pseudo-second-order kinetic model was also used to analyze data and it is given by:

$$\frac{t}{q_t} = \frac{1}{k_2 q_e^2} + \frac{t}{q_e} \tag{4}$$

where k_2 is the pseudo-second-order rate constant for the adsorption process.

2.6. Isotherm models

To obtain the adsorption isotherm, experiments were conducted at room temperature by 6 mg mL^{-1} of chitosan-coated magnetic nanoparticles with various initial concentrations of As(III), and results were fitted by adsorption isotherm models such as Langmuir and Freundlich models. The Langmuir isotherm model is based on monolayer adsorption and the bonding sites on the adsorbent have the same affinity for adsorption, due to which the adsorption occurs by chemical reaction [22]. The Langmuir isotherm is represented by the following equation:

$$\frac{C_e}{q_e} = \frac{C_e}{q_m} + \frac{1}{q_m K_L} \tag{5}$$

where q_e is the equilibrium adsorbate loading on the adsorbent in mg g^{-1}, C_e is the solute equilibrium concentration in mg L^{-1}, q_m is the ultimate capacity, and K_L is Langmuir constants. The values of q_m and K_L were determined from the slope and intercept of the linear plots of C_e/q_e vs. C_e.

The Freundlich isotherms model is based on a multilayer adsorption and assumes a heterogeneous surface which with the adsorption energy decreases with the surface coverage [23] and it is given by:

$$\mathrm{Ln}\, q_e = \frac{1}{n}\mathrm{Ln}\, C_e + \mathrm{Ln}\, K_F \tag{6}$$

where K_F and $1/n$ are Freundlich constants related to adsorption capacity and intensity of adsorption, respectively. The values of K and $1/n$ were determined from the slope and intercept of the linear plot of ln q_e vs. ln C_e.

3. Results and discussions

3.1. Characterizations of Chitosan-coated Fe_3O_4 nanoparticles

3.1.1. Transmission electron microscopy

Typical TEM images of naked and chitosan-coated Fe_3O_4 are shown in Fig. 1. Well-shaped spherical and uniform sizes of magnetic nanoparticles are observed. The mean diameter of naked Fe_3O_4 nanoparticles was 10 nm while the mean diameter of chitosan-coated nanoparticles was about 7 nm. This revealed that the chitosan grafting had resulted in the deagglomeration of secondary particles. This might be due to the change in the surface functional groups of the magnetic nanoparticles by the grafting of the chitosan. So, binding process leads to better distribution of chitosan-coated magnetic nanoparticles.

3.1.2. Dynamic light scattering and UV–vis spectra of magnetic nanoparticles

The hydrodynamic diameter distribution of naked and chitosan-coated magnetic nanoparticles in water prepared by the dynamic light scattering (DLS) technique is shown in Fig. 2. The mean hydrodynamic diameters of the naked and chitosan-coated magnetic nanoparticles were found to be 10.1 and 7.7 nm, respectively. In order to understand the dispersability of the nanoparticles in water, we have measured the DLS of the nanoparticles. It was indicated that the distributions of the resultant nanoparticles were narrow.

Fig. 3 shows the UV–visible absorption spectra of the suspension of naked and chitosan-coated nanoparticles. According to this graph, chitosan coating causes the change in the UV–vis spectra of Fe_3O_4 nanoparticles, and this confirms the binding of chitosan on Fe_3O_4 nanoparticles.

3.1.3. FTIR analysis

FTIR spectra of the pure Fe_3O_4, chitosan, and chitosan-coated magnetic nanoparticles were examined in the wave number range of 350–4,000 cm^{-1} to confirm the existence of the surface coating. The resulting graph is presented in Fig. 4. For pure Fe_3O_4 nanoparticles, the peak at 585 cm^{-1} corresponds to Fe–O–Fe

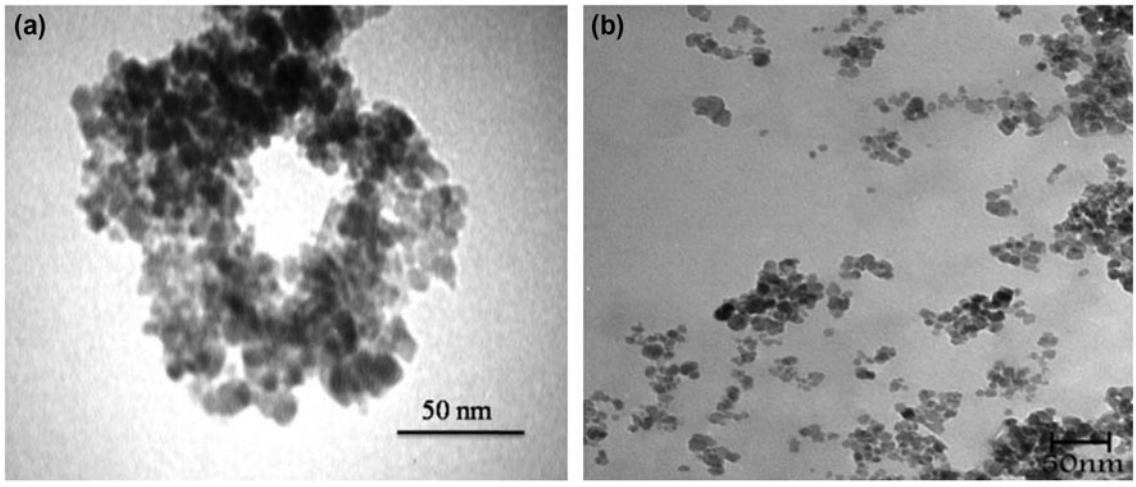

Fig. 1. TEM images of (a) the naked and (b) chitosan-coated Fe_3O_4 nanoparticles.

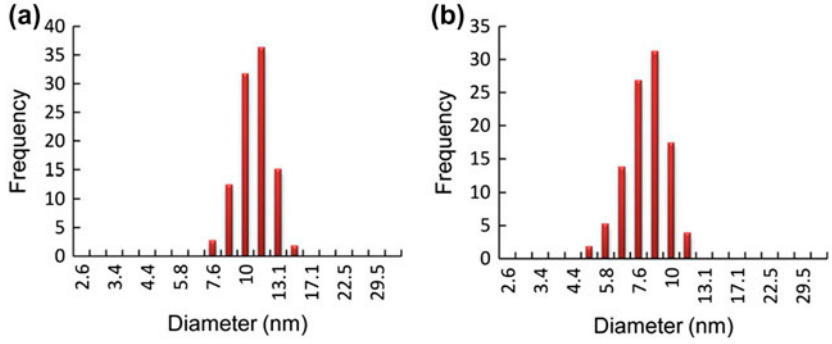

Fig. 2. DLS plots of (a) the naked and (b) chitosan-coated Fe_3O_4 nanoparticles.

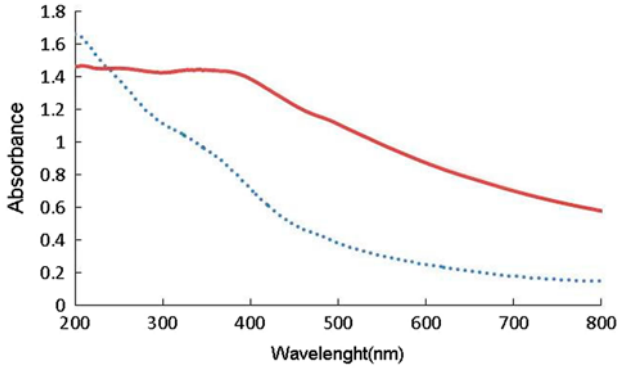

Fig. 3. UV–visible spectra of (Dot line) the naked and (Solid line) chitosan-coated Fe_3O_4 nanoparticles.

bond which is shifted to 607 cm^{-1} after surface modification with chitosan; for chitosan, the peak at 3,406 cm^{-1} is attributed to O–H and N–H stretching vibration, and C–O stretching vibration of the chitosan is obvious through peaks at 1,034 and 1,062 cm^{-1}. The peak at 1,434 cm^{-1} is typical of the C–N stretching vibration, and the peaks at 2,860 cm^{-1} corresponded to the C–H stretching vibrations. The characteristic adsorption bands appeared at 1,611 cm^{-1} correspond to N–H bending vibration (amine $–NH_2$) [24,25]. The FTIR spectra of chitosan-coated Fe_3O_4 indicated that chitosan and Fe_3O_4 were both presented in magnetic chitosan nanoparticles; in other words, the Fe_3O_4 magnetic nanoparticles were coated by the chitosan.

3.1.4. VSM analysis

The magnetic properties of the naked and chitosan-coated Fe_3O_4 nanoparticles were measured by VSM at room temperature, with the field sweeping from −10,000 to 10,000 Oe. In Fig. 5, the hysteresis loops that are characteristic of superparamagnetic behavior can be clearly observed for both naked and chitosan-coated magnetic nanoparticles. There was no

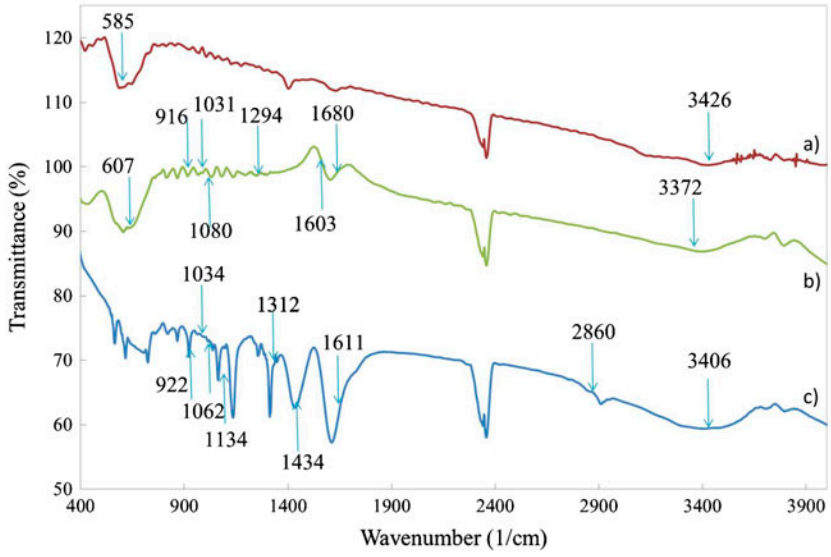

Fig. 4. FTIR spectra of (a) uncoated Fe_3O_4 magnetic nanoparticles, (b) chitosan-coated magnetic nanoparticles, and (C) chitosan.

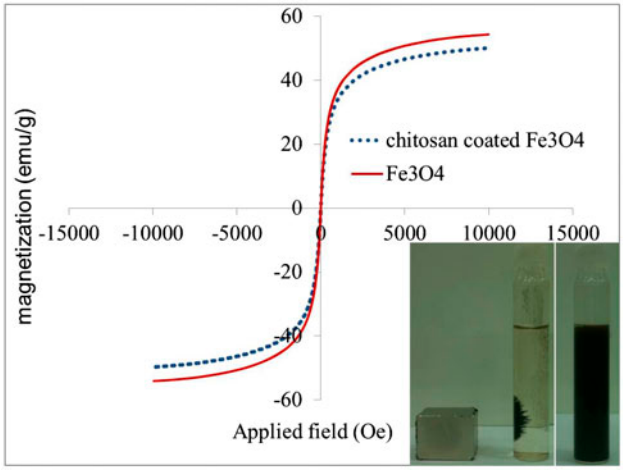

Fig. 5. Magnetic hysteresis curves of (solid line) the naked and (dot line) chitosan-coated Fe_3O_4 nanoparticles.

remanence and coercivity, suggesting that magnetic chitosan nanoparticles are superparamagnetic [24]. Materials with superparamagnetic behavior can be easily separated from the solution with the help of an external magnetic field (see Fig. 5, inset). The saturated magnetizations for Fe_3O_4 and chitosan-coated Fe_3O_4 nanoparticles are 54 and 50 μg^{-1}, respectively. Based on this feature, the chitosan-coated magnetic nanoparticles will be very useful for adsorption and separation operation.

3.1.5. Zeta-potential analysis

Zeta potential analysis was performed to investigate the surface net charge of nanoparticles. Chitosan is a linear polymer, chemically described as a poly(N glucosamine) with hydroxyl and amine groups present at the 2,3-, and 5-position in the glucose unit, respectively. The novel adsorption capacity of chitosan can be attributed to its functional groups. The hydroxyl groups increase the hydrophilicity of the polymer, which enables diffusion into the polymer network that allows adsorption from aquatic solutions. The hydroxyl and amino groups also have a high reactivity and can react with solutes in a number of different ways [26]. The high nitrogen content of chitosan makes up a large number of active sites that are subject to different chemical interactions in water solutions. The amine sites in their deprotonated form can bind metals through chelation mechanisms [26]. Zeta potential values of chitosan-bound Fe_3O_4 nanoparticles dispersed at acidic (pH 3) and basic (pH 9) media were measured. The results (Fig. 6) show negative values for basic and positive value at acidic media. It is expectable according to the isoelectric point of chitosan (at pH 6.3) [12] due to the presence of amine, carboxylic, and hydroxyl groups of chitosan.

3.2. Adsorption of arsenic onto chitosan-coated magnetic nanoparticles

3.2.1. Effects of initial pH on arsenic adsorption

The effect of pH values on arsenic adsorption by magnetite materials was investigated. The pH of

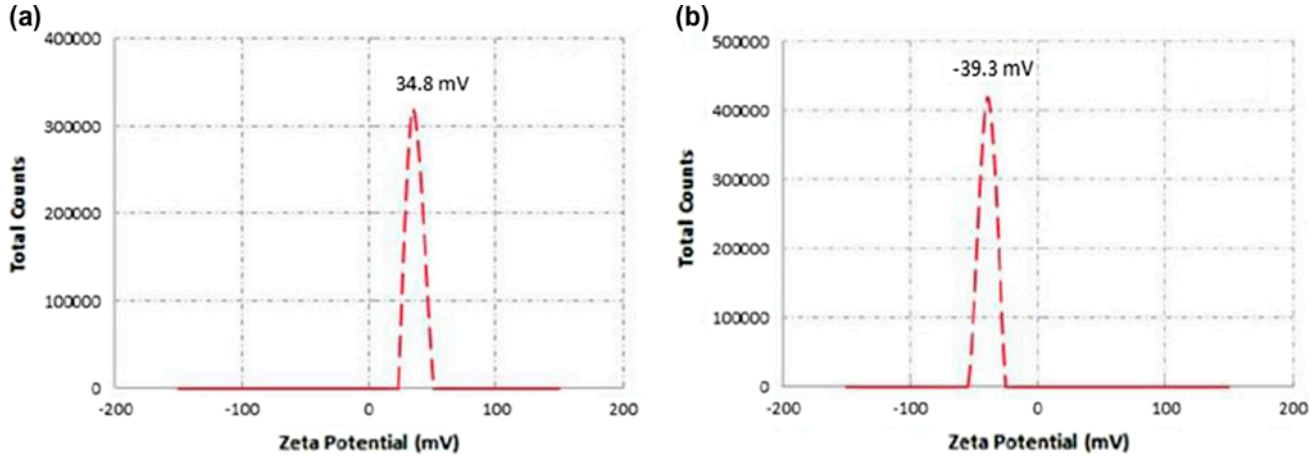

Fig. 6. Zeta potential distribution graphs of chitosan-bound Fe_3O_4 nanoparticles at (a) pH 3 (b) pH 9.

aqueous solution is an important factor in the adsorption process, because it affects the speciation of arsenic, chemical properties of adsorbate, and surface characteristics of the sorbents. The effect of initial pH on the removal efficiency of arsenic by chitosan-coated Fe_3O_4 nanoparticles at room temperature and the initial arsenic concentration of 50 ppm are illustrated in Fig. 7. As mentioned in Section 3.1.5, the zeta potential values show that the net charge on the adsorbent surface can be altered by changing in pH values from acidic to basic media. Acidic pH values were avoided because the acid environments could lead to partial dissolution of chitosan polymer and may make the coated nanoparticles unstable. So, the pH values range between 8 and 11 was chosen. According to the literature [27], at pH < 9.2, trivalent arsenic mainly existed as uncharged species (H_3AsO_3) in water while, chitosan has made a negative net charge on the nanoparticle surface at pH > 6.3 [12]. So, the adsorption of arsenite on the nanoparticles may be due to the hydrogen bond formation between As(III) and chitosan layer on the nanoparticle surface [28]. At pH > 9.2, negatively charged species of arsenic ($H_2AsO_3^-$) will be formed that caused the decrease in the adsorption of arsenic on the nanoparticles surface, because of electrostatic repulsion.

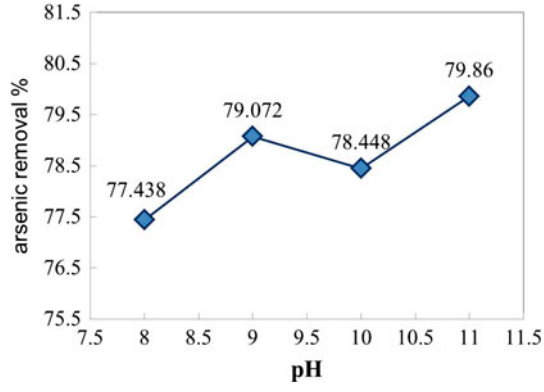

Fig. 7. Effect of pH on arsenic removal by chitosan-coated Fe_3O_4 nanoparticles.

As can be seen in Fig. 7, the adsorption amount of arsenic increased by varying pH value from 8 to 9 and then decrease after 9, that is, due to the formation of negatively charged form of arsenite. An undesirable increase in removal efficiency was observed on pH 11 that may be due to the complex formation between adsorbent and arsenite. Generally, arsenite removal efficiency is not a strong function of pH [12,27]. Finally, pH 9 was selected as the optimum pH for arsenic adsorption using chitosan-coated Fe_3O_4 was selected.

3.2.2. Adsorption kinetics

The adsorption kinetics describes the solute uptake rate. The adsorption of As(III) on chitosan-coated magnetic nanoparticles was studied at pH 9 with time ranging from 5 to 90 min, as shown in Fig. 8. Based on Fig. 8, it can be seen that the adsorption occurs rapidly which may be due to the abundant active sites on the adsorbents and the greater concentration gradient. More than 60% of the arsenite was adsorbed by chitosan-coated magnetic nanoparticles within the first 5 min. However, later on, with a gradual decrease in the number of active sites, the uptake of As(III) ions becomes very slow. This is a common behavior with adsorption processes and has been repeatedly reported in other studies [15].

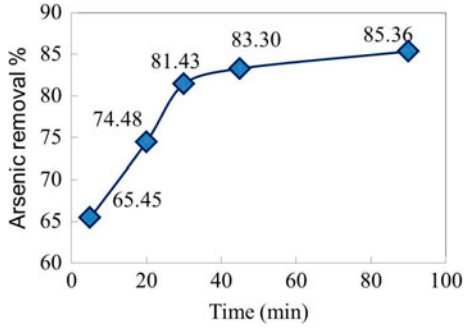

Fig. 8. The effect of contact time on the arsenic removal by the chitosan-coated Fe_3O_4 nanoparticle.

The experimental data of adsorption for As (III) onto chitosan-coated magnetic nanoparticles were analyzed using Lagergren pseudo-first-order and pseudo-second-order kinetic models (Eqs. (3) and (4)). By plotting ln $(q_e - q_t)$ vs. t, according to the pseudo-first order model (the figure has not been shown here) q_e, K_1 and R_2 could be calculated. In the same manner, q_e, K_2 and R_2 could be calculated from the slope and intercept of the plot of t/q_t vs. t according to the pseudo-second order model (Fig. 9). All calculated kinetic parameters have been shown in Table 1. From the parameters listed in Table 1, it is obvious that the adsorption kinetic follows the pseudo-second-order kinetic model which is better than the other model, because of its higher correlation coefficients (R^2). Also equilibrium adsorption capacities determined by the pseudo-second-order model ($q_{e,cal} = 7.2993$) were in agreement with the experimentally determined equilibrium adsorption capacities ($q_{e,exp}$ = 7.1133). These findings indicated that the pseudo-second-order adsorption mechanism was predominant. Also, this point suggests that arsenic adsorption process probably be controlled by the chemisorption process [29].

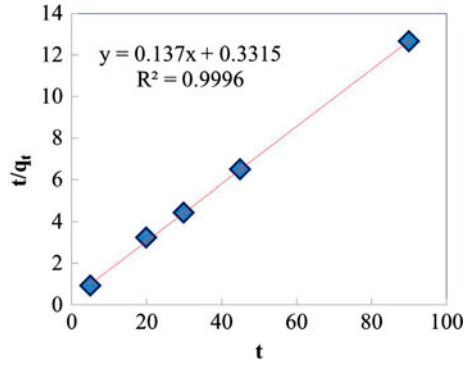

Fig. 9. Pseudo-second-order kinetics for adsorption of As (III) by chitosan-coated Fe_3O_4 nanoparticles.

3.2.3. Influence of amount of chitosan-coated magnetic nanoparticles

The effect of adsorbent dosage on arsenite adsorption capacity and removal efficiency was investigated and the results are shown in Fig. 10. Evaluating the optimum dosage of chitosan-coated magnetic nanoparticles needed some adsorption studies of As (III) onto chitosan-coated magnetic nanoparticles using 50 ppm As (III) treated with varying chitosan-coated magnetic nanoparticles dosage. In this test, the concentration of arsenic aqueous solution was kept at 50 ppm. As shown in Fig. 10, it is clear that the removal efficiency of arsenic increases with the increase in the chitosan-coated Fe_3O_4 nanoparticle dosage. The percentage of the removal increases markedly from 42.4 to 90.6% by increasing the amount of the chitosan-coated Fe_3O_4 adsorbent from 2 to 10 mg mL^{-1}. while the adsorption amount per unit of adsorbent decreased with increasing amount of chitosan-coated Fe_3O_4. This observation can be explained by the fact that the number of available adsorption sites increased by increasing adsorbent dose, thus leading to the increase of adsorbed arsenite amount. While unsaturation of adsorption sites through the adsorption process contributed to the decrease in equilibrium uptake with increasing adsorbent dose. Of course, it may be also due to aggregation which is resulted from high sorbent dose. Such aggregation would lead to a decrease in total surface area of the sorbent and an increase in diffusional path length [29,30]. Fig. 10 indicates that a sorbent concentration of 8 mg mL^{-1} would lead to a best removal percentage and the best sorbent capacity.

3.2.4. Effects of initial As(III) concentration on As(III) adsorption

As mentioned above, chitosan-coated magnetic nanoparticles provided good capacity for As(III) at pH 9 at room temperature. The adsorption isotherm of arsenic was obtained by varying the initial concentration of As(III) at the range values from 1 to 100 ppm. It can be observed from Fig. 11 that removal efficiency of As(III) decreases with increasing the initial As(III) concentration. Therefore, As (III) removal is related inversely to initial arsenic concentrations. This was expected due to the fact that for a fixed adsorbent dosage, the total available adsorption sites are limited, thus the percentage of adsorbate removal decreases corresponding to an increased initial adsorbate concentration. The reason for the decrease in As(III) adsorption efficiency at higher initial concentrations may be due to reducing active adsorption sites.

Table 1
Adsorption kinetic parameters of As(III) onto chitosan-coated magnetic nanoparticles

Pseudo-first-order			Pseudo-second-order			
k_1(min^{-1})	$q_{e,cal}$ (mg g^{-1})	R^2	$q_{e,exp}$ (mg g^{-1})	k_2 (g mg^{-1} min)	$q_{e,cal}$ (mg g^{-1})	R^2
0.0594	2.3812	0.9689	7.1133	0.0566	7.2993	0.9996

Table 2
Adsorption isotherm parameters for As(III) adsorption on chitosan-coated magnetic nanoparticles at pH 9

Langmuir model			Freundlich model		
q_m	K_L	R^2	n	K_F	R^2
10.5042	0.1413	0.9938	0.5884	1.7256	0.97

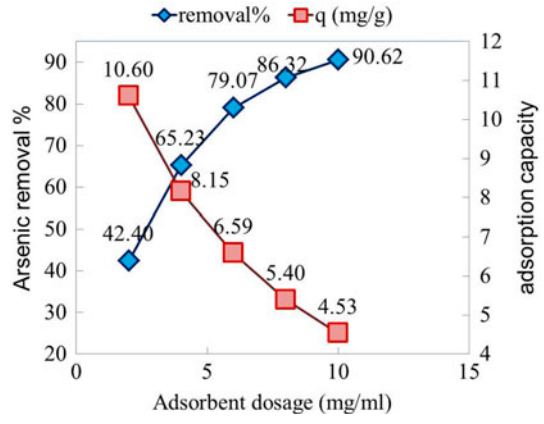

Fig. 10. The effect of chitosan-coated Fe_3O_4 nanoparticle adsorbent dosage on arsenic efficiencies and adsorption capacity of magnetic nanoparticles.

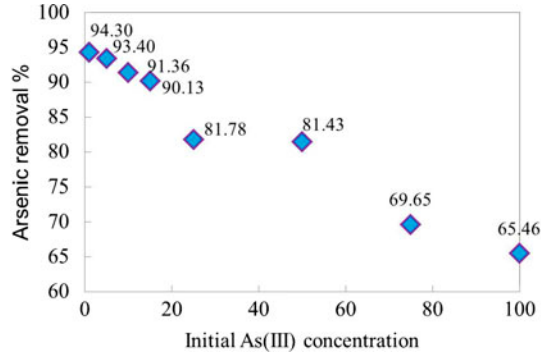

Fig. 11. The effect of initial As(III) concentration on arsenic removal efficiency of magnetic nanoparticles.

3.2.5. Adsorption equilibrium isotherms

To understand the adsorption mechanism of As(III) ions on the chitosan-coated magnetic nanoparticles, adsorption equilibrium was investigated at pH 9 with an initial As(III) concentration with the range of 1–100 ppm at room temperature. Studying adsorption isotherm is important in the purification of wastewater, because it provides some information about adsorption reactions. Adsorption equilibrium, indicating the capacity of the adsorbent, is described by adsorption isotherm which is characterized by certain constants whose values express the surface properties and affinity of the adsorbent [19,31]. Here, the equilibrium data were fitted by Langmuir and Freundlich isotherm equations to describe the equilibrium between adsorbed As(III) on chitosan-coated magnetic nanoparticles (q_e) and As(III) in solution (C_e) at a constant temperature. Fig. 12 illustrates the isotherms models for As(III) adsorption on chitosan-coated magnetic nanoparticles and the isotherm parameters are shown in Table 2. The high values of correlation coefficients, R^2, indicate that the adsorption isotherms of As(III) onto the chitosan-coated magnetic nanoparticles better fit Langmuir model than Freundlich model, and assumes that it is a monolayer adsorption process.

Also, the maximum sorption capacity obtained from the Langmuir isotherm was 10.5 mg g^{-1}. This result is comparable with the adsorption capacity of the other similar sorbents reported in literature. This remarkable adsorption capacity makes chitosan-coated magnetic nanoparticles one of the best adsorbents for the removal of As(III) from aqueous solutions [1,23,32].

3.2.6. Effect of chitosan coating on arsenic adsorption

To investigate the effect of coating material on adsorption of trivalent arsenic, the adsorption capacity of chitosan-coated magnetic nanoparticles and the synthesized naked Fe_3O_4 were compared. By comparing the arsenic removal efficiency by Fe_3O_4 with and without the coating in Table 3, we can see that the removal efficiency of As(III) by Fe_3O_4 coated with chitosan are

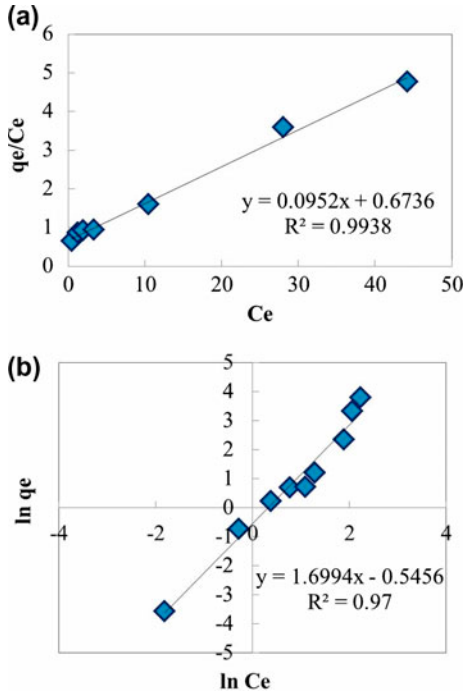

Fig. 12. The Langmuir (a) and Freundlich (b) isotherm plots for As(III) adsorption by chitosan-coated magnetic nanoparticles at pH 9.

higher than the bare ones. Hereby, the use of chitosan as coating of Fe_3O_4 magnetic nanoparticle can enhance the arsenic removal. One reason is that the coating can prevent Fe_3O_4 particles from aggregating in adsorption process and increase the effective adsorption area and functional groups present in the adsorbent, resulting in highly enhancement of adsorption capacity.

3.2.7. Desorption experiments

One of the most important factors in applying adsorbents is their ability for reusing in another cycles. Generally, regeneration of adsorbents was done using some kinds of acidic, basic, or aqueous solvents. Here, to evaluate the possibility of regeneration of the chitosan-coated magnetic nanoparticles, desorption experiments were conducted. For this purpose, nanoparticles were used for arsenic removal from the fresh solution (initial As (III) concentration = 20 ppm). After adsorption of arsenic by the nanoparticles during 30 min, the nanoparticles were separated from the solution and kept for the second step. Then, the separated nanoparticles which adsorbed As(III) ions from the solution should be dispersed in the elution solvents. Hot water, 0.1 M NaOH, and 0.1 M H_2SO_4 solutions were chosen as elution solvent to investigate the desorption of As (III) from the nanoparticles. After a certain time, the nanoparticles were separated from elution solvents by applying the magnet, and the solvents were analyzed for measuring their arsenic content. The results were shown in Table 4 as the desorption percentage. As can be seen, neither acidic nor basic media cannot desorb the arsenic ions from the nanoparticles more than 40% (for H_2SO_4). These results are supported by similar research [5]. So, it can be claimed that arsenic adsorption was obeyed from a chemisorption rule, in which many of adsorbed arsenic cannot be desorbed after eluting. In the second step, regenerated nanoparticles were used for a new removal process and the results were shown in the last column in Table 4 as the recovery percentage.

To investigate if, using acidic media can cause removing chitosan layer from nanoparticle surface or not, FTIR spectrum (Fig. 13) was collected for eluted nanoparticles. Fig. 13 indicates the presence of four peaks in wave number range about 1,100–1,700 cm^{-1} (the region in the circle), which are related to the amine functional groups of chitosan (see Section 3.1.3). So, it can be claimed that these regenerated nanoparticles still maintained their chitosan layer.

3.2.8. Real samples

To evaluate the effect of chitosan-coated magnetic nanoparticles on adsorption of arsenic from real samples, several arsenic adsorption experiments with chitosan-coated magnetic nanoparticles were conducted. The three real water samples were obtained from the villages of Kurdistan province and an industrial sample from petroleum industry spiked to an arsenic concentration of 10 ppm. To determinate As(III) concentration in real samples, As(III) concentration was measured using ICP-MS. The initial

Table 3
Comparison of the removal efficiency of As(III) using naked and Chitosan Coated Fe_3O_4 Nanoparticle

Absorbance	Concentration (ppm)	Removal efficiency
Naked Fe_3O_4 nanoparticles	10	74.59
Chitosan coated Fe_3O_4 nanoparticles	10	87.46

Table 4
Results of regeneration and recovery of chitosan-coated magnetic nanoparticles on arsenic removal

Elution solvent	% Adsorption	Time of elution	% Desorption	% Recovery
H_2SO_4	89.71	3 h	40.56	68.85
NaOH	90.59	3 h	33.90	76.435
Hot water	86.62	30 min	7.7	–

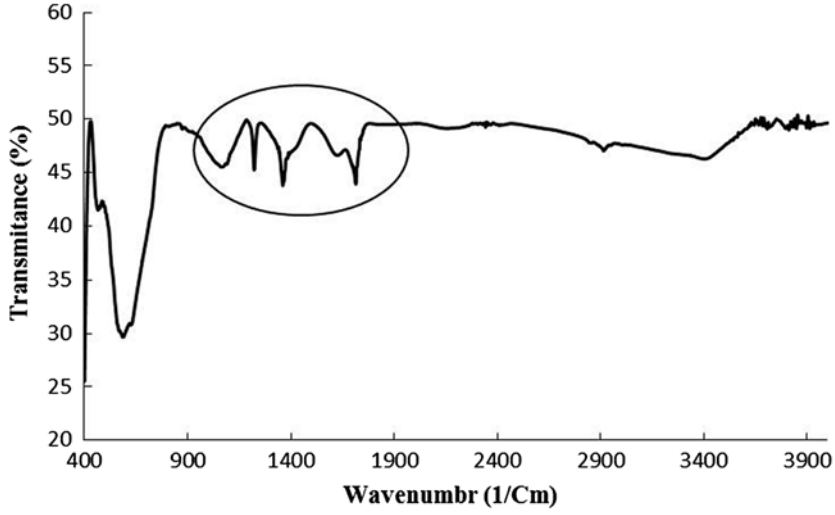

Fig. 13. FTIR spectrum of regenerated magnetic nanoparticles which have been eluted by H_2SO_4 previously.

Table 5
Removal efficiency of As(III) in real samples by chitosan-coated Fe_3O_4 magnetic nanoparticles

Real sample	Initial As(III) (ppm)	Spiked As(III) (ppm)	% Removal
Gavandak	0.578	–	95.67
Ghochagh	0.186	10	87.28
Babagorgor	0.133	10	90.45
Industrial water	0.0047	10	91.7

concentration of As(III) in real samples and the removal efficiencies of As(III) after treatment with chitosan-coated magnetic nanoparticles were listed in Table 5. The observed removal efficiencies for As(III) from real samples were about 95%. These values were not influenced by the commonly coexisted ions in real samples water. According to Table 5, it is clear that the amount of arsenic in the studied sample after treatment was lower than drinking water standards of WHO.

4. Conclusions

In this study, a new magnetic chitosan nanoadsorbent was developed by modifying the surface of magnetic nanoparticles for arsenic removal. These nanoadsorbents have magnetic properties of Fe_3O_4 nanoparticles and adsorption properties of chitosan. The TEM images showed that the chitosan-coated Fe_3O_4 nanoparticles were monodisperse and have a mean diameter of about 7 nm. These magnetic nanoadsorbents can effectively be used to remove As(III) from aqueous solution, and modifying the surface Fe_3O_4 by chitosan can enhance the arsenic adsorption. Various factors affecting the uptake behavior such as contact time, pH, amount of chitosan-coated magnetic nanoparticles, and initial concentration of As(III) were evaluated. The adsorption behavior obeyed the Langmuir adsorption isotherm model with a maximum monolayer adsorption capacity of 10.5 mg g^{-1} at room

temperature. Results of this research suggest that the chitosan-coated magnetic nanoparticles would be effective for the removal of heavy metal ions from wastewater using the technology of magnetic separation. Compared with the similar research [15], using chitosan-coated magnetic nanoparticles instead of chitosan bead or other forms of chitosan:magnetic nanoparticle composite is more efficient because of faster kinetic adsorption reaction.

Acknowledgment

We acknowledge the nanotechnology research Institute of Shiraz University and the ministry of science and technology as providers of financial sum, facilities, contributors, etc.

References

[1] L. Feng, M. Cao, X. Ma, Y. Zhu, Ch. Hu, Superparamagnetic high-surface-area Fe_3O_4 nanoparticles as adsorbents for arsenic removal, J. Hazard. Mater. 217–218 (2012) 439–446.
[2] L. Dong, P.V. Zinin, J.P. Cowen, L.Ch. Ming, Iron coated pottery granules for arsenic removal from drinking water, J. Hazard. Mater. 168 (2009) 626–632.
[3] A. Figoli, A. Cassano, A. Criscuoli, M.S.I. Mozumder, M.T. Uddin, M.A. Islam, E. Drioli, Influence of operating parameters on the arsenic removal by nanofiltration, Water Res. 44 (2010) 97–104.
[4] A.H. Barati, A. Maleki, M. Alasvand, Multi-trace elements level in drinking water and the prevalence of multi-chronic arsenical poisoning in residents in the west area of Iran, Sci. Total Environ. 408 (2010) 1523–1529.
[5] Ch.Ch. Chen, Y.Ch. Chung, Arsenic removal using a biopolymer chitosan sorbent, J. Environ. Sci. Health, Part A 41 (2006) 645–658.
[6] M.I. Litter, M.E. Morgada, J. Bundschuh, Possible treatments for arsenic removal in Latin American waters for human consumption, Environ. Pollut. 158 (2010) 1105–1118.
[7] H. Saitua, R. Gil, A.P. Padilla, Experimental investigation on arsenic removal with a nanofiltration pilot plant from naturally contaminated groundwater, Desalination 274 (2011) 1–6.
[8] Y.Y. Park, T. Tran, Y.H. Lee, Y.I. Nam, G. Senanayake, M.J. Kim, Selective removal of arsenic(V) from a molybdate plant liquor by precipitation of magnesium arsenate, Hydrometallurgy 104 (2010) 290–297.
[9] M. Sen, A. Manna, P. Pal, Removal of arsenic from contaminated groundwater by membrane-integrated hybrid treatment system, J. Membr. Sci. 354 (2010) 108–113.
[10] B. Pakzadeh, J.R. Batista, Surface complexation modeling of the removal of arsenic from ion-exchange waste brines with ferric chloride, J. Hazard. Mater. 188 (2011) 399–407.
[11] P.K. Srivastava, A. Vaish, S. Dwivedi, D. Chakrabarty, N. Singh, R.D. Tripathi, Biological removal of arsenic pollution by soil fungi, Sci. Total Environ. 409 (2011) 2430–2442.
[12] V.M. Boddu, K. Abburi, J.L. Talbott, E.D. Smith, R. Haasch, Removal of arsenic (III) and arsenic (V) from aqueous medium using chitosan-coated biosorbent, Water Res. 42 (2008) 633–642.
[13] A. Gupta, V.S. Chauhan, N. Sankararamakrishnan, Preparation and evaluation of iron–chitosan composites for removal of As(III) and As(V) from arsenic contaminated real life groundwater, Water Res. 43 (2009) 3962–3870.
[14] D. Mohan, C.U. Pittman Jr., Arsenic removal from water/wastewater using adsorbents—A critical review, J. Hazard. Mater. 142 (2007) 1–53.
[15] D.D. Gang, B. Deng, L.Sh. Lin, As(III) removal using an iron-impregnated chitosan sorbent, J. Hazard. Mater. 182 (2010) 156–161.
[16] A.Z.M. Badruddoza, G.S.S. Hazel, K. Hidajat, M.S. Uddin, Synthesis of carboxymethyl-β-cyclodextrin conjugated magnetic nano-adsorbent for removal of methylene blue, Colloid. Surf. A: Physicochem. Eng. Aspects 367 (2010) 85–95.
[17] A.Z.M. Badruddoza, A.S.H. Tay, P.Y. Tan, K. Hidajat, M.S. Uddin, Carboxymethyl-β-cyclodextrin conjugated magnetic nanoparticles as nano-adsorbents for removal of copper ions: Synthesis and adsorption studies, J. Hazard. Mater. 185 (2011) 1177–1186.
[18] W.S.W. Ngah, L.C. Teong, M.A.K.M. Hanafiah, Adsorption of dyes and heavy metal ions by chitosan composites: A review, Carbohydr. Polym. 83 (2011) 1446–1456.
[19] A. Gupta, M. Yunus, N. Sankararamakrishnan, Zerovalent iron encapsulated chitosan nanospheres—A novel adsorbent for the removal of total inorganic Arsenic from aqueous systems, Chemosphere 86 (2012) 150–155.
[20] A. Khodabakhshi, M.M. Amin, M. Mozaffari, Synthesis of magnetite nanoparticles and evaluation of its efficiency for arsenic removal from simulated industrial wastwater, Iran. J. Environ. Health Sci. Environ. 8 (2011) 189–200.
[21] Y.Ch. Chang, D.H. Chen, Preparation and adsorption properties of monodisperse chitosan-bound Fe_3O_4 magnetic nanoparticles for removal of Cu(II) ions, J. Colloid Interf. Sci. 283 (2005) 446–451.
[22] S. Zhang, X. Li, J.P. Chen, Preparation and evaluation of a magnetite-doped activated carbon fiber for enhanced arsenic removal, Carbon 48 (2010) 60–67.
[23] Y. Tian, M. Wu, X. Lin, P. Huang, Y. Huang, Synthesis of magnetic wheat straw for arsenic adsorption, J. Hazard. Mater. 193 (2011) 10–16.
[24] C. Yuwei, W. Jianlong, Preparation and characterization of magnetic chitosan nanoparticles and its application for Cu(II) removal, Chem. Eng. J. 168 (2011) 286–292.
[25] O. Osuna, K.G. Jauregui, J.G.G. Lozano, I.M.d.la.G. Rodrıguez, A. Ilyna, E.D.B. Castro, H. Saade, R.U.G. Lopez, Chitosan-coated magnetic nanoparticles with low chitosan content prepared in one-step, J. Nanomater. 7 (2012) 1–7.
[26] G. Crini, Recent developments in polysaccharide-based materials used as adsorbents in wastewater treatment, Prog. Polym. Sci. 30 (2005) 38–70.

[27] D.D. Gang, B. Deng, L. Lin, As(III) removal using an iron-impregnated chitosan sorbent, J. Hazard. Mater. 182 (2010) 156–161.
[28] C.C. Chen, Y.C. Chung, Arsenic removal using a biopolymer chitosan sorbent, J. Environ. Sci. Health A 41 (2006) 645–658.
[29] H.Y. Mei, Ch. Man, H.Zh. Bo, Effective removal of Cu (II) ions from aqueous solution by amino-functionalized magnetic nanoparticles, J. Hazard. Mater. 184 (2010) 392–399.
[30] M. Namdeo, S.K. Bajpai, Chitosan–magnetite nanocomposites (CMNs) as magnetic carrier particles for removal of Fe(III) from aqueous solutions, Colloid. Surf. A: Physicochem. Eng. Aspects 320 (2008) 161–168.
[31] Q. Peng, Y. Liu, G. Zeng, W. Xu, C. Yanga, J. Zhang, Biosorption of copper(II) by immobilizing Saccharomyces cerevisiae on the surface of chitosan-coated magnetic nanoparticles from aqueous solution, J. Hazard. Mater. 177 (2010) 676–682.
[32] S. Luther, N. Borgfeld, J. Kim, J.G. Parsons, Removal of arsenic from aqueous solution: A study of the effects of pH and interfering ions using iron oxide nanomaterials, Microchem. J. 101 (2010) 30–36.